A Schnyder-Type Drawing Algorithm for 5-Connected Triangulations

Olivier Bernardi, Éric Fusy, Shizhe Liang

A Schnyder-type drawing algorithm for 5-connected triangulations*

Olivier Bernardi[1], Éric Fusy[2], and Shizhe Liang[1]

[1] Department of Mathematics, Brandeis University, Waltham MA, USA
{bernardi,shizhe1011}@brandeis.edu
[2] CNRS/LIGM, Université Gustave Eiffel, Champs-sur-Marne, France
eric.fusy@univ-eiffel.fr

Abstract. We define some Schnyder-type combinatorial structures on a class of planar triangulations of the pentagon which are closely related to 5-connected triangulations. The combinatorial structures have three incarnations defined in terms of orientations, corner-labelings, and woods respectively. The wood incarnation consists in 5 spanning trees crossing each other in an orderly fashion. Similarly as for Schnyder woods on triangulations, it induces, for each vertex, a partition of the inner triangles into face-connected regions (5 regions here). We show that the induced barycentric vertex-placement, where each vertex is at the barycenter of the 5 outer vertices with weights given by the number of faces in each region, yields a planar straight-line drawing.

Keywords: Schnyder structures, barycentric drawing, 5-connected triangulations

1 Introduction

In 1989, Walter Schnyder showed that planar triangulations can be endowed with remarkable combinatorial structures, which now go by the name of *Schnyder woods* [24]. A Schnyder wood of a planar triangulation is a partition of its inner edges into three trees, crossing each other in an orderly manner; see Figure 1(a) for an example. In [25], Schnyder used his structures to define an elegant algorithm to draw planar triangulations with straight edges [25].

In this article we study an analogue of Schnyder woods for triangulations of the pentagon, which we call *5c-woods*, and we show that such structures exist if and only if cycles of length less than 5 have no vertex in their interior (a property closely related to 5-connectedness). We then use these structures to define a graph-drawing algorithm in the spirit of Schnyder's algorithm.

A disadvantage of our algorithm compared to Schnyder's original algorithm (and to algorithms such as [6,7,8,11,15,18,21] using an underlying combinatorial

* OB was partially supported by NSF Grant DMS-2154242. EF was partially supported by the project ANR19-CE48-011-01 (COMBINÉ), and the project ANR-20-CE48-0018 (3DMaps).

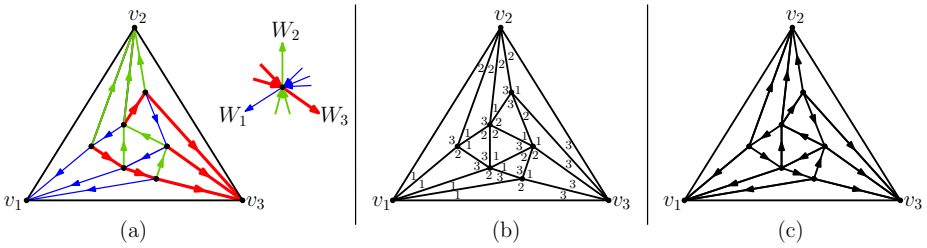

Fig. 1. (a) A Schnyder wood (with the local condition at inner vertices), (b) the corresponding corner labeling, (c) the corresponding 3-orientation.

structure or shelling order to define a vertex-placement) is that it does not yield a *grid-drawing* algorithm, that is, a vertex placement where the coordinates are integers bounded by a linear function of the number of vertices of the graph. Nevertheless, we stress some nice features of our algorithm: it can be implemented in linear time, it respects rotational symmetries, and the worst-case vertex resolution (minimal distance between vertices) is better than in Schnyder's drawing. On the examples we have tested, our algorithm seems to output aesthetically pleasant drawings; see Figure 7 for an example.

Our article is organized as follows. All the combinatorial results are presented in Section 2. We start by defining the 5c-structures for triangulations of the pentagon (see Figure 2 for an example, which parallels Figure 1). We give three different incarnations of these structures (5c-woods, 5c-labelings, 5c-orientations), we explain the equivalence between them, state the exact condition for their existence, and point to the appendix for detailed proofs and the description of a linear-time construction algorithm. The drawing algorithm is then presented in Section 3. Together with the proof of planarity of the drawing, this section includes a discussion of the drawing properties mentioned above, and some open questions.

Let us mention that the 5c-structures presented here are closely related to the *quasi-Schnyder structures* which we introduced in [3]. The quasi-Schnyder structures are a far-reaching generalization of Schnyder woods (encompassing regular edge labelings [17], and Schnyder decompositions considered in [1]), and in the case of triangulations of the pentagon, these structures can be identified with the 5c-structures which are the focus of the present article. Focusing on triangulations of the pentagon allows us to provide a simplified presentation, both in terms of definitions and proofs, and also to define an additional incarnation in terms of woods. Let us add that the quasi-Schnyder structures for triangulations of the square coincide (after simplifications) with *regular edge labelings* [17] (a.k.a. *transversal structures* [15]), and the quasi-Schnyder structures for triangulations coincide (after simplifications) with the classical Schnyder woods [24]. Another combinatorial structure which bears some resemblance to 5c-structures are the five color forests introduced in [13] that are related to pentagon contact

representations. As we will explain in Remark 1, one can easily construct a five color forest from a 5c-structure (but the opposite is not true).

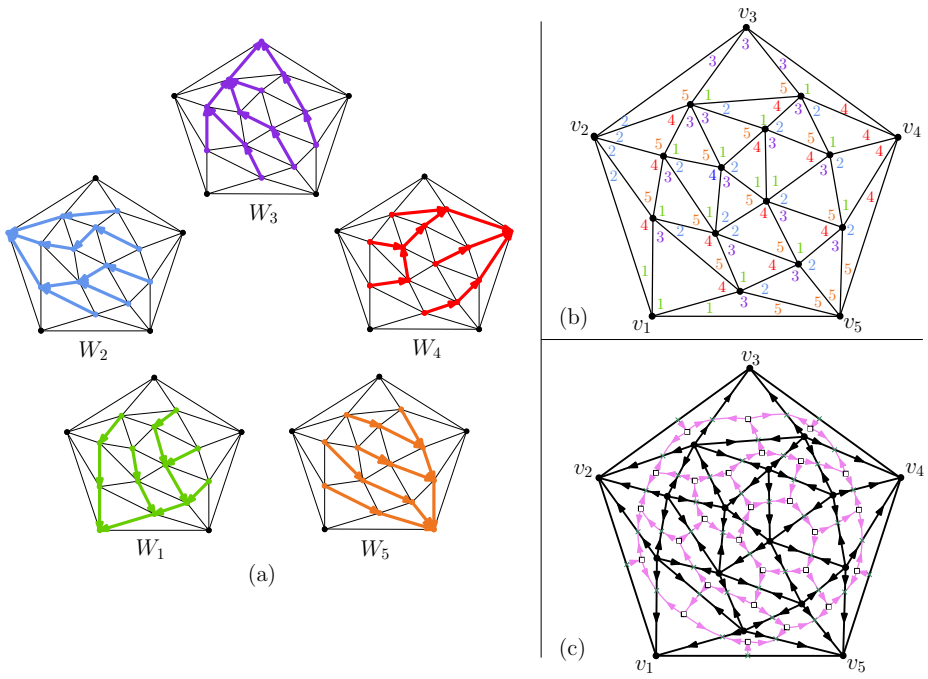

Fig. 2. The three incarnations of 5c-structures. (a) A 5c-wood $\mathcal{W} = (W_1, \ldots, W_5)$. (b) The 5c-labeling $\mathcal{L} = \Theta^{-1}(\mathcal{W})$. (c) The 5c-orientation $\mathcal{O} = \Phi(\mathcal{L})$.

2 Schnyder structures for triangulations of the pentagon

2.1 Definitions about triangulations

A *plane map* is a connected planar graph G with a fixed planar embedding. The *faces* of G are the connected components of $\mathbb{R}^2 \backslash G$. The *outer face* is the unique unbounded face, the other faces are called *inner*. An *arc* of G is an edge with a choice of direction. We use the notation $\{u, v\}$ for an edge connecting the vertices u and v, and (u, v) for an arc oriented from u to v. The two arcs on an edge are called *opposite*. A *corner* is a sector delimited by two consecutive edges around a vertex. Corners, vertices, edges and arcs are called *outer* when they are incident to the outer face, and *inner* otherwise.

A *triangulation of the pentagon*, or *5-triangulation* for short, is a plane map such that the inner faces have degree 3 and the outer face contour is a simple cycle

of length 5. The outer vertices of a 5-triangulation are denoted by $v_1, v_2, \ldots, v_5$ in clockwise order around the outer face; see Figure 2. A *5c-triangulation* is a 5-triangulation such that every cycle with at least one vertex in its interior has length at least 5. Note that 5c-triangulations have no loops nor multiple edges. In the terminology of [3], 5c-triangulations are the 5-triangulations which are *quasi 5-adapted*. It is easy to check that a 5-triangulation G is a 5c-triangulation if and only if the graph G' obtained from G by adding the edges $\{v_i, v_{i+2}\}$ for all $i \in \{1, 2, \ldots, 5\}$ is 5-connected (in particular 5-connected 5-triangulations are 5c-triangulations). Let us mention lastly that deleting a vertex of degree 5 from a 5-connected planar triangulation (such a vertex necessarily exists, by the Euler relation) yields a 5c-triangulation; hence the algorithm presented in Section 3 for 5c-triangulations gives a way to draw 5-connected planar triangulations (upon seeing the deleted vertex as a vertex at infinity).

The *primal-dual completion* of a plane map G is the map G^+ obtained by inserting a vertex v_e in the middle of each edge e, inserting a vertex v_f in each inner face f, and then connecting v_f to all edge-vertices corresponding to the edges incident to f. An example is shown in Figure 2(c). The vertices of G^+ corresponding to faces (resp. edges) of G are called *dual vertices* (resp. *edge-vertices*), while the original vertices of G are called *primal vertices*.

2.2 Three incarnations of Schnyder structures on 5-triangulations

In this section we present three different incarnations of Schnyder-type structures on 5-triangulations and define bijections between them. The incarnations are called *5c-woods*, *5c-labelings* and *5c-orientations* respectively. The conditions defining these structures are indicated in Figure 3. We start by discussing 5c-orientations, an example of which is presented in Figure 2(c).

Definition 2.1 *Given a 5-triangulation G, a* 5c-orientation *of G is an orientation of the inner edges of the primal-dual completion G^+ of G satisfying the following conditions:*

(O0) The outer primal vertices have outdegree 0.
(O1) The inner primal vertices have outdegree 5*, the dual vertices have outdegree* 2*, and the edge-vertices (including the outer ones) have outdegree* 1.

The definition of 5c-orientations is illustrated in the top row of Figure 3.

Next, we define *5c-labelings*, an example of which is presented in Figure 2(b). A *corner labeling* of a 5-triangulation G is an assignment of a *label* in $[1:5] := \{1, 2, 3, 4, 5\}$ to each inner corner of G. For two corners c and c' with labels i and i' respectively, we call *label jump* from c to c' the integer $\delta \in \{0, 1, 2, 3, 4\}$ such that $i + \delta \equiv i' \pmod 5$.

Definition 2.2 *Given a 5-triangulation G, a* 5c-labeling *of G is a corner labeling of G satisfying the following conditions:*

(L0) For all $i \in [1:5]$, every inner corner incident to v_i has label i.

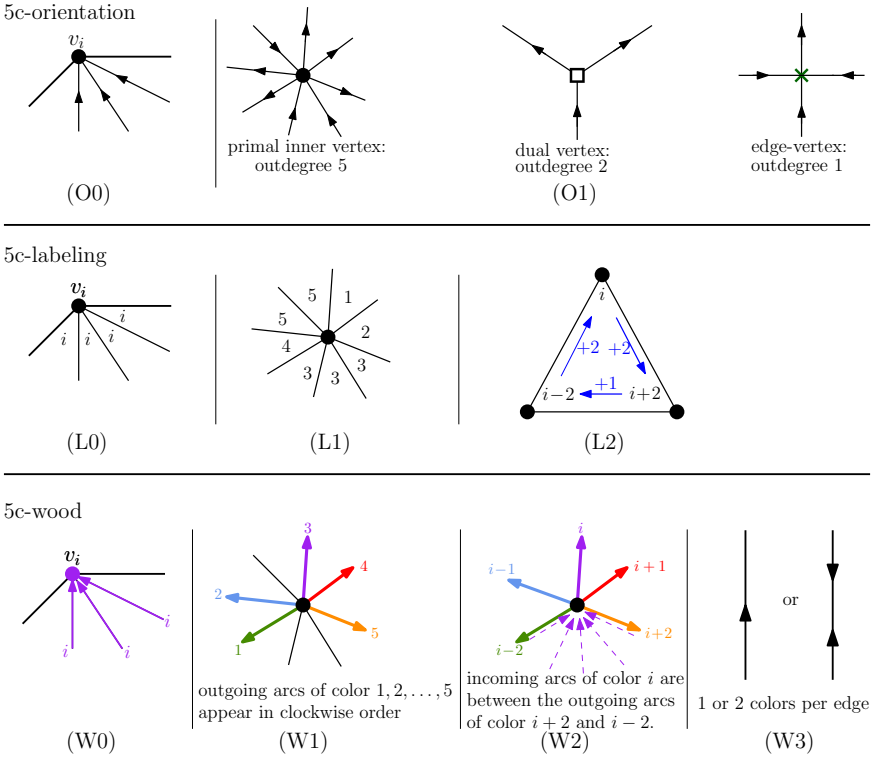

Fig. 3. Definition of 5c-structures. Top row: Conditions defining 5c-orientations. Middle row: Conditions defining 5c-labelings. Bottom row: Conditions defining 5c-woods.

(L1) Around every inner vertex, the incident corners form 5 non-empty intervals I_1, I_2, I_3, I_4, I_5 in clockwise order, with all corners in I_i having label i .

(L2) Around every inner face, in clockwise order, there are two label jumps equal to 2 and one label jump equal to 1.

Conditions (L0-L2) are illustrated in Figure 3 (middle row).

Next, we define a bijection Φ between 5c-labelings and 5c-orientations. The mapping Φ is represented in Figure 4(a).

Definition 2.3 *Given a 5c-labeling $\mathcal{L}$ of G, we define an orientation $\Phi(\mathcal{L})$ on G^+ as follows. First we note that there is a one-to-one correspondence between the inner corners of G and the inner faces of G^+, hence we interpret $\mathcal{L}$ as a labeling of the inner faces of G^+. Let $e = \{v, x\}$ be an inner edge of G^+, where v is either a primal or dual vertex, and x is an edge-vertex.*

– *If v is a primal vertex, and f^- and f^+ are the faces incident to e in G^+ in clockwise order around v, then e is oriented toward v if and only if the label jump from f^- to f^+ is 0 (i.e., f^- and f^+ have the same label).*

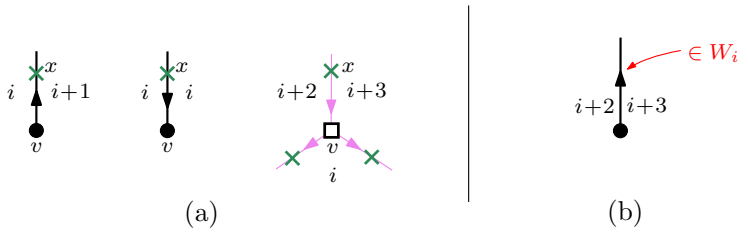

Fig. 4. Rules giving the bijections between 5c-orientations, 5c-labelings, and 5c-wood. Vertices of G are represented by solid black dots, whereas dual vertices are represented by squares, and edge-vertices are represented by crosses. (a) Local rule giving the bijection Φ from 5c-labelings to 5c-orientations. (b) Local rule giving the bijection Θ from 5c-labelings to 5c-woods.

– *If v is a dual vertex, and f^- and f^+ are the faces incident to e in G^+ in clockwise order around v, then e is oriented toward v if and only if the label jump from f^- to f^+ is 1.*

Lemma 2.4 *The map Φ is a bijection between the set $\mathbf{L}_G$ of 5c-labelings on G and the set $\mathbf{O}_G$ of 5c-orientations on G.*

The proof of Lemma 2.4 can be found in Appendix A.1.

The third incarnation is called *5c-woods*, where the structure is encoded by a tuple $\mathcal{W} = (W_1, ..., W_5)$ of directed trees. An example is given in Figure 2(a).

It is sometimes convenient to think of the tuple $\mathcal{W} = (W_1, ..., W_5)$ as a coloring in $[1:5]$ of the inner arcs of G. We say that an inner arc a of G has a color i if this arc belongs to W_i. The precise definition of a 5c-wood is as follows.

Definition 2.5 *Given a 5-triangulation G, a* 5c-wood *of G is a tuple $\mathcal{W} = (W_1, ..., W_5)$ of disjoint subsets of inner arcs, satisfying the following conditions:*

(W0) No arc in $\mathcal{W}$ starts at an outer vertex, and those ending at the outer vertex v_i have color i for all $i \in [1:5]$.
(W1) Every inner vertex v has a unique outgoing arc of color i, for $i \in [1:5]$, and these arcs appear in clockwise order around v.
*(W2) Let v be an inner vertex with incident outgoing arcs $a_1, ..., a_5$ of colors $1, ..., 5$, respectively. Any arc a of color i having terminal vertex v appears weakly between a_{i+2} and a_{i+3} in clockwise order around v (*weakly *means that a may be the arc opposite to a_{i+2} or a_{i+3}).*
(W3) Every inner edge has at least one color.

Conditions (W0-W3) are illustrated in the bottom row of Figure 3. We will prove later (see Proposition 3.1) that for any 5c-wood $\mathcal{W} = (W_1, \ldots, W_5)$ the set of arcs W_i is acyclic for all i. Given that every inner vertex has outdegree 1 in W_i, it follows that W_i is a tree spanning all the inner vertices and the outer

vertex v_i, and oriented toward the root-vertex v_i (that is, every arc in W_i is oriented from child to parent when v_i is taken as the root of the tree W_i).

Now we define a bijection Θ between 5c-labelings and 5c-woods. The mapping Θ is represented in Figure 4(b).

Definition 2.6 *Given a 5c-labeling $\mathcal{L}$ of G, we define a tuple $\Theta(\mathcal{L}) = (W_1, ..., W_5)$ of subsets of inner arcs of G (interpreted as a partial arc coloring) as follows: an inner arc $a = (u, v)$ receives color i if the labels of the corners on the left and on the right of a (at u) are $i + 2$ and $i + 3$, respectively; the arc a has no color if the two labels are equal.*

Lemma 2.7 *The map Θ is a bijection between the set $\mathbf{L}_G$ of 5c-labelings on G and the set $\mathbf{W}_G$ of 5c-woods on G.*

The proof of Lemma 2.7 can be found in Appendix A.2.

Remark 1. We can give a fourth incarnation of 5c-structures, as a representation of the 5-triangulation by a contact system of "soft pentagons" as indicated in Figure 5. Let G be a 5-triangulation. A *soft pentagon contact representation* of G is a collection of interior-disjoint "soft pentagons" (the sides of which are curves rather than straight-line segments) inside a regular "outer pentagon", with vertices of each pentagon labeled 1 to 5 in clockwise order such that

- the side $[i + 2, i + 3]$ of the outer pentagon corresponds to the outer vertex v_i of G, for $i \in [1 : 5]$,
- the soft pentagons correspond to the inner vertices of G,
- contacts between pentagons correspond to the inner edges of G,
- all the pentagon contacts occur between a soft pentagon vertex of label $i \in [1 : 5]$ and either the side labeled $[i+2, i+3]$ of another soft pentagon (vertex-to-side contact), or the vertex $i+2$ or $i+3$ of another soft pentagon (vertex-to-vertex contact), or the side labeled $[i + 2, i + 3]$ of the outer pentagon (outer contact, always vertex-to-side).

A soft pentagon contact representation is *complete* if every vertex of every soft pentagon has a contact. It is easy to see that the 5c-woods of G are in bijection with its complete soft pentagon contact representations. This is illustrated in Figure 5. This topological interpretation of 5c-woods allows us to compare them to the *five color forests* introduced in [13]. For a 5-triangulation G these structures correspond to general (potentially incomplete) soft pentagon contact representations without vertex-to-vertex contact. In particular, one can easily turn any 5c-wood into a five color forest, upon resolving each vertex-to-vertex contact into a vertex-to-side contact. At the level of the 5c-wood (interpreted as a collection of arcs colored in $[1 : 5]$), this amounts to deleting one colored arc for each edge of G bearing 2 colored arcs. Note however that it is usually not possible to turn a five color forest into a 5c-wood. Indeed, five color forests exist for any simple 5-triangulation, while (as stated below) 5c-woods only exist for 5c-triangulations.

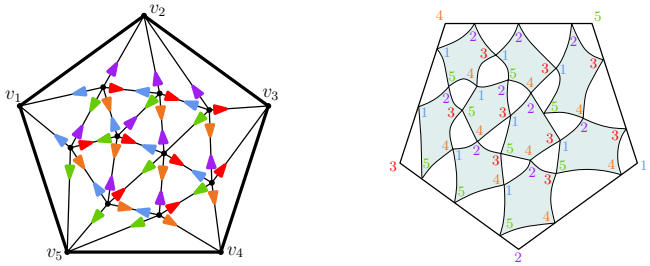

Fig. 5. Left: A 5c-wood. Right: The corresponding (complete) soft pentagon contact representation.

2.3 Existence and computation of Schnyder structures

We now state our main result on 5c-structures (where we include the already obtained bijective statements).

Theorem 2.8 *A 5-triangulation G admits a 5c-wood (resp. 5c-labeling, 5c-orientation) if and only if G is a 5c-triangulation. In this case, the sets of 5c-woods, 5c-labelings and 5c-orientations of G are in bijection. Moreover, a 5c-wood (resp. 5c-labeling, 5c-orientation) of a 5c-triangulation can be computed in linear time in the number of vertices.*

We have already stated in Section 2.2 that, for any 5-triangulation G, the sets of 5c-woods, 5c-labelings and 5c-orientations of G are in bijection. Moreover, it is clear that these bijections can be performed in linear time in the number of vertices. It thus remains to show that a 5-triangulation admits a 5c-orientation if and only if it is a 5c-triangulation, and that, in this case, a 5c-orientation can be computed in time linear. We already proved this existence (and algorithmic) result in [3] within the larger framework of *quasi-Schnyder structures*. Since there are many layers to the proof given in [3], we sketch a more direct proof (and construction algorithm) in Appendix A.3.

3 Graph drawing algorithm for 5c-triangulations

3.1 Paths and regions

In this section we explain how a 5c-wood gives rise to paths and regions associated to each vertex of a 5c-triangulation; see Figure 6(b).

Let G be an undirected graph. A *biorientation* of G is an arbitrary subset of arcs of G (so that each edge of G is oriented in either 0, 1 or 2 directions). A biorientation is *acyclic* if it contains no simple directed cycle, with the convention that two opposite arcs (coming from the same edge oriented in 2 directions) do not constitute a simple cycle. Suppose now that G is a 5c-triangulation, and let $\mathcal{W} = (W_1, \dots, W_5)$ be a 5c-wood. For $i \in [1:5]$, we denote by W_i^- the set of arcs obtained by reversing the arcs in W_i (that is, taking the opposite arcs).

Proposition 3.1 *Let $\mathcal{W} = (W_1, \dots, W_5)$ be a 5c-wood of G. For all $i \in [1:5]$, the biorientation $\mathcal{O}_i = W_i \cup W_{i-1} \cup W_{i+1} \cup W_{i-2}^- \cup W_{i+2}^-$ is acyclic. Consequently, for each pair $j, k \in [1:5]$, the biorientation $W_j \cup W_k^-$ is acyclic.*

The proof of Proposition 3.1 can be found in Appendix A.4. An example is shown in Figure 6(a).

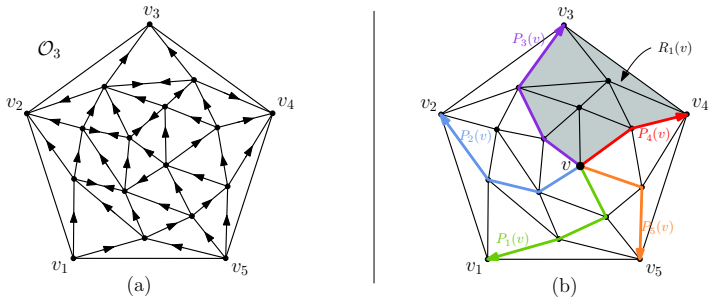

Fig. 6. (a) The biorientation $\mathcal{O}_3$ for the 5c-wood represented in Figure 2. (b) The paths $P_1(v), \dots, P_5(v)$ and the region $R_1(v)$ for the 5c-wood in Figure 2.

As mentioned in Section 2, Proposition 3.1 implies that in any 5c-wood $\mathcal{W} = (W_1, \dots, W_5)$ of G, each set W_i is a tree directed toward the outer vertex v_i. For an inner vertex v of G, we denote by $P_i(v)$ the directed path from v to v_i in W_i. These paths are indicated in Figure 6(b). Proposition 3.1 implies that the paths $P_1(v), \dots, P_5(v)$ have no vertex in common except v (since if $P_j(v)$ and $P_k(v)$ had a vertex in common, the biorientation $W_j \cup W_k^-$ would contain a directed cycle). We denote by $R_i(v)$ the region enclosed by the simple cycle made of the outer edge (v_{i+2}, v_{i-2}) together with the paths $P_{i-2}(v)$ and $P_{i+2}(v)$. See Figure 6(b) for an example.

3.2 Graph drawing algorithm

For convenience, we extend the definition of $R_i(v)$ for v an outer vertex by declaring $R_i(v_i) = G$ for all $i \in [1:5]$, and $R_i(v_j) = \{v_j\}$ for all $j \neq i$. For a vertex v of G and for $i \in [1:5]$, the *size* of $R_i(v)$, denoted by $|R_i(v)|$, is the number of inner faces in $R_i(v)$. Letting n be the number of vertices of G, the Euler relation implies that G has $2n-7$ inner faces. Let $\alpha_i(v) := |R_i(v)|/(2n-7)$. Since the inner faces of G are partitioned among the 5 regions, we have $\sum_{i=1}^{5} \alpha_i(v) = 1$.

The *5c-barycentric drawing algorithm* then consists of the following steps:

1. Draw a regular pentagon $(v_1, v_2, v_3, v_4, v_5)$ (in clockwise order).
2. Place each vertex v at the barycenter $\sum_{i=1}^{5} \alpha_i(v) v_i$.
3. Draw each edge of G as a segment connecting the corresponding points.

An output of this algorithm is represented in Figure 7. In all our drawings, the outer pentagon is drawn with the edge $\{v_1, v_5\}$ as an horizontal bottom segment.

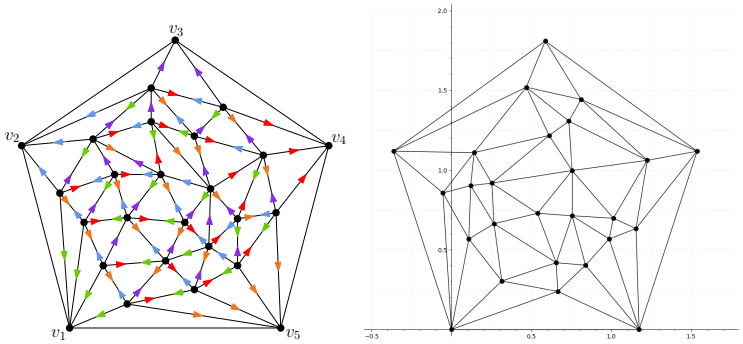

(a) (b)

Fig. 7. (a) A 5c-wood $\mathcal{W} = (W_1, \ldots, W_5)$ of a 5c-triangulation (the sets of arcs in $W_1, \ldots, W_5$ are represented by arrows of 5 different colors). (b) The drawing of G obtained by applying the 5c-barycentric drawing algorithm with $\mathcal{W}$ as input.

Theorem 3.2 *For each 5c-triangulation G with n vertices, the 5c-barycentric drawing algorithm yields a planar straight-line drawing of G, which can be computed in $O(n)$ operations.*

Remark 2. Compared to Schnyder's algorithm [25] and to Tutte's spring embedding [27], it is important here that the 5 outer vertices are placed so as to form a regular pentagon, and we use this property in our proof of planarity.

We will prove the planarity of the 5c-barycentric drawing in the next section. The time-complexity analysis can be found in Appendix A.5.

3.3 Proof of planarity

The proof of planarity in Theorem 3.2 crucially relies on a property (illustrated in the right drawing of Figure 9 and to be established in Lemma 3.4) stating that the directions of the arcs of each color from an inner vertex are constrained to be in certain cones. As a first step we show the following "half-plane property", illustrated in Figure 8.

Lemma 3.3 *Let G be a 5c-triangulation endowed with a 5c-wood. In the associated 5c-barycentric drawing, for $i \in [1:5]$, let $\overrightarrow{V_i}$ be the vector connecting the center of the outer pentagon (i.e. the center of the circle circumscribed to that*

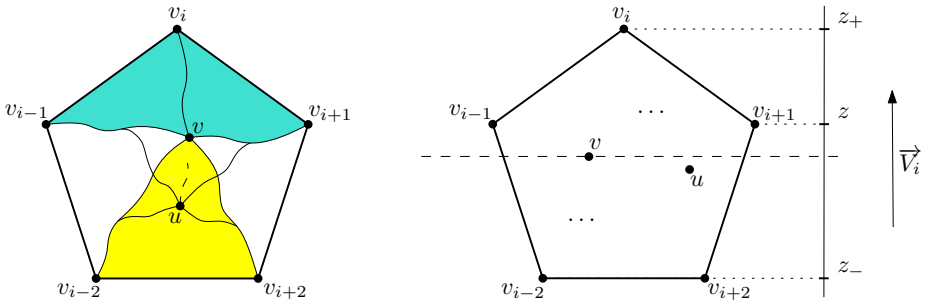

Fig. 8. Left: Situation for two vertices $u \neq v$ such that $u \in R_i(v)$, where the interior of $R_i(v)$ is shown in yellow, and the interior of $R_{i-2,i+2}(v)$ is shown in blue. Right: In the 5c-barycentric drawing, u is in the half-plane "below" v upon rotating the drawing such that $\overrightarrow{V_i}$ points upward.

pentagon) to the outer vertex v_i. Then, for any vertices $u \neq v$ of G such that $u \in R_i(v)$, we have $\overrightarrow{V_i} \cdot \overrightarrow{vu} < 0$, where $\overrightarrow{vu}$ is the vector connecting v to u in the 5c-barycentric drawing.

Proof. For each vertex w and each subset S of $[1:5]$, we use the extended notation $R_S(w) = \cup_{i\in S} R_i(w)$, and $\alpha_S(w) = \sum_{i\in S} \alpha_i(w)$. We then observe the following containment relations (see Figure 8):

$$R_i(v) \supset R_i(u), \quad R_{i-2,i+2}(v) \subset R_{i-2,i+2}(u).$$

The second relation is due to the fact (which follows from Condition (W2) of 5c-woods) that, whenever $P_{i-1}(u)$ (resp. $P_{i+1}(u)$) leaves the region $R_i(v)$, it occurs just after visiting a vertex on $P_{i-2}(v)$ (resp. on $P_{i+2}(v)$).

Defining $z_- < z < z_+$ as

$$z_- = \overrightarrow{V_i} \cdot \overrightarrow{V_{i-2}} = \overrightarrow{V_i} \cdot \overrightarrow{V_{i+2}}, \quad z = \overrightarrow{V_i} \cdot \overrightarrow{V_{i-1}} = \overrightarrow{V_i} \cdot \overrightarrow{V_{i+1}}, \quad z_+ = \overrightarrow{V_i} \cdot \overrightarrow{V_i},$$

and letting $r = \alpha_{i-2,i+2}(u) - \alpha_{i-2,i+2}(v)$, $s = \alpha_{i-1,i+1}(u) - \alpha_{i-1,i+1}(v)$, and $t = \alpha_i(u) - \alpha_i(v)$, we then have

$$\begin{aligned}\overrightarrow{vu} \cdot \overrightarrow{V_i} &= \sum_{k=1}^{5} (\alpha_k(u) - \alpha_k(v)) \overrightarrow{V_k} \cdot \overrightarrow{V_i} \\ &= r\, z_- + s\, z + t\, z_+ \\ &= r\, z_- + (-r-t) z + t\, z_+ = r\,(z_- - z) + t\,(z_+ - z),\end{aligned}$$

where from the 2nd to 3rd line we use the identity $r + s + t = 1 - 1 = 0$. The above containment relations ensure that $t < 0$ and $r > 0$, so that $\overrightarrow{vu} \cdot \overrightarrow{V_i} < 0$. □

Lemma 3.4 *Let G be a 5c-triangulation endowed with a 5c-wood. For v an inner vertex of G, and for $i \in [1:5]$, let u be the terminal vertex of the arc of*

color i from v. Then, in the 5c-barycentric drawing of G, the angle between the vector $\overrightarrow{V_i}$ (defined as in Lemma 3.3) and the vector $\overrightarrow{vu}$ is in the open interval $(-\frac{3\pi}{10}, \frac{3\pi}{10})$ (see Figure 9 right).

Proof. Clearly $u \in P_i(v) = R_{i-2}(v) \cap R_{i+2}(v)$. Hence, by Lemma 3.3 we have $\overrightarrow{vu} \cdot \overrightarrow{V_{i-2}} < 0$ and $\overrightarrow{vu} \cdot \overrightarrow{V_{i+2}} < 0$, which is equivalent to the stated property. □

Remark 3. Lemmas 3.3 and 3.4 are the analogues of well-known properties of Schnyder drawings for simple triangulations, where $(-\frac{3\pi}{10}, \frac{3\pi}{10})$ is to be replaced by $(-\frac{\pi}{6}, \frac{\pi}{6})$ in Lemma 3.4. A difference here is that the property as stated does not immediately guarantee that the outgoing edges of an inner vertex are in clockwise order in the drawing, since the cones for adjacent colors overlap. However, as we now show, the property is actually enough to ensure planarity, and thus the cyclic ordering of edges around a vertex is preserved in the drawing.

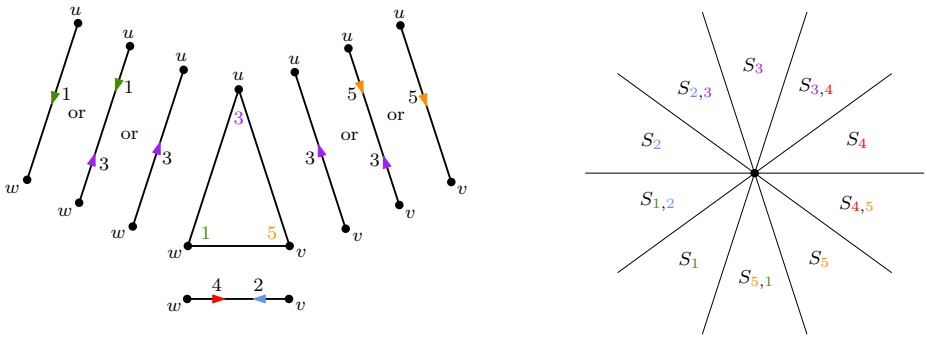

Fig. 9. Left: Possible cases for the colors of arcs around an inner face with corner labels $1, 3, 5$. Right: Conditions of Lemma 3.4 (a sector S_i can only have the arc of color i from the shown vertex, a sector $S_{i,j}$ can only have the arcs of colors in $\{i, j\}$).

To show that the drawing is planar, by a known topological argument (see e.g. [9, Lem.4.4]), it suffices to show that each inner face is *properly represented*, that is, represented as a non-degenerated triangle that is not flipped (indeed, this condition ensures that the function mapping a point p inside the enclosing pentagon to the number $n(p)$ of triangles covering it is locally constant, hence has to be equal to 1 everywhere). In other words, if the corner labels are $i, i+2, i+3$ in clockwise order around an inner face, we have to show that these corners are seen in the same cyclic order in the triangle representing the face. It is clear that the 5 inner faces incident to the 5 outer edges are properly represented, so we can focus on inner faces incident to 3 inner edges. Let us treat the case $i = 3$ (the other cases can be treated symmetrically), where the vertices at the corners $3, 5, 1$ are respectively denoted u, v, w. Given the conditions defining

corner-labelings, and the bijection between 5c-woods and 5c-labelings, it is easy to check that the following holds (see Figure 9 left):

- The arc (v, w) has color 2, and the arc (w, v) has color 4.
- The arc (v, u) has color 3 if colored, the arc (u, v) has color 5 if colored, and at least one of these two arcs is colored.
- The arc (w, u) has color 3 if colored, the arc (u, w) has color 1 if colored, and at least one of these two arcs is colored.

By Lemma 3.4, and using the notation of Figure 9 right, the arc (v, w) is in sector $S_2 \cup S_{1,2}$ from v, and the arc (w, v) is in sector $S_4 \cup S_{4,5}$ from w (the fact that $\{v, w\}$ is a straight segment in the drawing excludes sectors $S_{2,3}$ and $S_{3,4}$ respectively). If the arc (v, u) is colored (with color 3), then it is in sector $S_{2,3} \cup S_3 \cup S_{3,4}$ from v, hence the directed angle from (v, u) to (v, w) around v is in the open interval $(0, \pi)$, so that the face (u, v, w) is properly represented. Similarly, if the arc (w, u) is colored (with color 3), then the directed angle from (w, v) to (w, u) around w is in the open interval $(0, \pi)$, so that the face (u, v, w) is properly represented. Finally, if none of the arcs (v, u) or (w, u) is colored, then the arc (u, w) has color 1, and the arc (u, v) has color 5. Assume for contradiction that the face (u, v, w) is not properly represented. Then the directed angle from (u, w) to (u, v) around u is not in the open interval $(0, \pi)$. Given Lemma 3.4, these two arcs have to be in $S_{5,1}$ from u, that is, the arc (w, u) is in S_3 from w and the arc (v, u) is in S_3 from v. But then, the angle from (w, v) to (w, u) around w is in the open interval $(\pi/5, 4\pi/5)$, so that the face (u, v, w) is properly represented. This concludes the proof of planarity in Theorem 3.2.

3.4 Variations and other properties

We discuss here some variants (weighted faces, vertex-counting) and aesthetic properties of the drawing, and end with some open questions.

Variants of the embedding algorithm. As in the case of Schnyder's algorithm [14], one can give a *weighted version* of the 5c-barycentric drawing algorithm. In this version, each inner face is assigned a positive weight, and $\alpha_i(v)$ is the total weight of inner faces in $R_i(v)$, divided by the total weight of inner faces. The proof of Lemma 3.4 and the proof of planarity extend verbatim. Moreover, as in [25, Sec.7], a vertex-counting variant can also be given, upon changing $|R_i(v)|$ to be the number of vertices in $R_i(v) \backslash P_{i-2}(v)$, and using $\alpha_i(v) = |R_i(v)|/(n-1)$, with n the number of vertices of G. The relevant inequalities to prove Lemma 3.3 become, for $u \neq v$ such that $u \in R_i(v)$,

$$|R_i(v)| \geq |R_i(u)|, \quad |R_{i-2,i+2}(v)| < |R_{i-2,i+2}(u)|.$$

(Note that, even if $R_i(v) \supset R_i(u)$, here we may have $|R_i(v)| = |R_i(u)|$ when u, v are part of a triangular face (v, u, w) such that u is the end of the arc of color $i-2$ and w is the end of the arc of color $i+2$ from v.) Hence, Lemma 3.4 still holds, which as before implies planarity.

Symmetries. Compared to Tutte's spring embedding [27] (and similarly as for Schnyder's drawing), the drawing algorithm (either in its face-counting or vertex-counting version) can display rotational symmetries, but not mirror symmetries. Precisely, there is a canonical 5c-wood corresponding to the *minimal 5c-orientation*, that is, the unique 5c-orientation with no counterclockwise directed cycle. If G is invariant by a rotation of order 5, then so is the minimal 5c-orientation, and so is the corresponding 5c-wood under a shift of the arc colors (and indices of the outer vertices) by 1. Thus, the drawing obtained using this canonical 5c-wood displays the rotational symmetry.

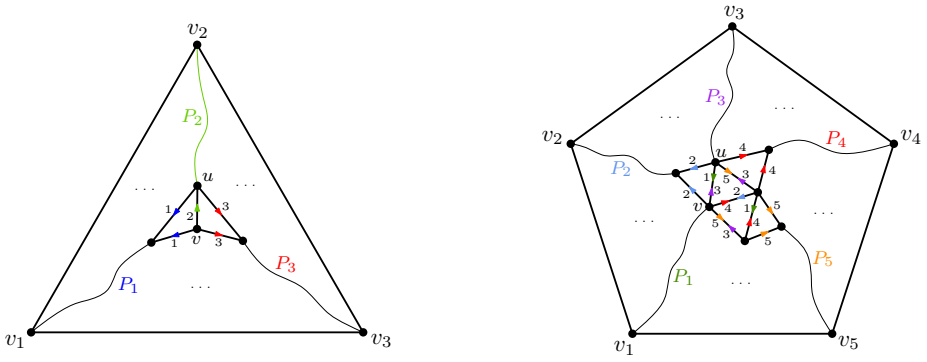

Fig. 10. The configuration (up to rotation and mirror) of vertex-pairs (u, v) of smallest possible distance in Schnyder's drawing (left) and in our drawing (right).

Quality of the drawing. Besides the fact that the family of triangulations is more restricted, an obvious disadvantage of our algorithm compared to Schnyder's one (and also to straight-line drawings using transversal structures [15], or using shelling orders [8,7,18,22,21]) is that we can not use an affine transformation to turn the drawing into one on a regular square-grid of linear width and height[3]. Let us however discuss a parameter (vertex resolution) for which our algorithm brings some improvement. For $n \geq 1$, we let $\mu_3(n)$ (resp. $\mu_5(n)$) denote the smallest possible distance between vertices over Schnyder's drawings on simple triangulations with n vertices (resp. over our 5c-barycentric drawings on 5-connected triangulations with n vertices), assuming the drawing is normalized to have circumscribed circle of radius 1. Below we use complex numbers to represent points in the plane. Let $\omega_3 = e^{2i\pi/3}$ (resp. $\omega_5 = e^{2i\pi/5}$). For a vector $\boldsymbol{\delta} = (\delta_1, \delta_2, \delta_3) \in \mathbb{Z}^3$ (resp. $\boldsymbol{\delta} = (\delta_1, \delta_2, \delta_3, \delta_4, \delta_5) \in \mathbb{Z}^5$) whose components add up to 0, we define the *modulus* $||\boldsymbol{\delta}||$ of $\boldsymbol{\delta}$ as the modulus $|z|$ of the complex number $z = \sum_{i=1}^{3} \delta_i \omega_3^i$ (resp. $z = \sum_{i=1}^{5} \delta_i \omega_5^i$). The vector $\boldsymbol{\delta}$ is called *possible* if there

[3] If we use an affine transformation to have v_1, v_2 and v_5 placed at $(0, 0)$, $(0, 1)$ and $(1, 0)$ respectively, then we get a drawing with vertex-coordinates in $\mathbb{Q}(\sqrt{5})$.

is a vertex pair (u, v) in a Schnyder's drawing (resp. in our drawing) such that the number of faces in $R_i(u)$ minus the number of faces in $R_i(v)$ equals δ_i for $i \in \{1, 2, 3\}$ (resp. for $i \in [1 : 5]$), in which case the distance between u and v in the drawing is $||\boldsymbol{\delta}||/(2n-5)$ (resp. is $||\boldsymbol{\delta}||/(2n-9)$).

As shown in Figure 10 (and following an easy case inspection), the possible $\boldsymbol{\delta}$ of smallest modulus (up to dihedral permutation of the entries) for Schnyder's drawing is $(-1, 2, -1)$, of modulus $d_3 = 3$, and for our drawing is $(-2, -1, 3, 1, -1)$, of modulus $d_5 \approx 5.97$. Thus (for n large enough) we have $\mu_3(n) = \frac{d_3}{2n-5}$, and $\mu_5(n) = \frac{d_5}{2n-9}$. Hence, the vertices are better kept away from each other in our drawing, the worst-case distance being increased by a factor $d_5/d_3 \approx 1.99$ (to have a comparison over the same objects, we note that $\mu_3(n)$ is also attained by drawings of 5-connected triangulations with n vertices, for n large enough).

In the vertex-counting variant, the possible $\boldsymbol{\delta}$ of smallest modulus (up to cyclic permutation of the entries) in Schnyder's algorithm is now $(0, 1, -1)$, of modulus $d'_3 = \sqrt{3} \approx 1.73$, and in our drawing is $(-1, -1, 1, 1, 0)$, of modulus $d'_5 \approx 3.08$ (these are again attained by the patterns shown in Figure 10). Then we have (for n large enough) $\mu_3(n) = \frac{d'_3}{n-1}$ and $\mu_5(n) = \frac{d'_5}{n-2}$, so that the worst-case distance is increased by a factor $d'_5/d'_3 \approx 1.78$ (in both algorithms the vertex-counting variant brings a slight improvement over the face-counting version).

Open questions: We conclude with some open questions:

Question 1. Can 5c-woods, and the 5c-barycentric algorithm, be generalized to 5-connected plane graphs in the spirit of the extension of Schnyder woods, and drawing algorithm, to 3-connected planar graphs [6,10,11,20]?

Question 2. Can 5c-woods be used to define a graph drawing algorithm for the dual of 5c-triangulations (possibly with bent edges but restrictions on the directions of the edge segments). Such algorithms are known for the dual of triangulations [12,20], the dual of irreducible triangulations of the 4-gon [17], and the dual of quadrangulations [1,4,26].

Question 3. Is there a shelling procedure on 5c-triangulations to output a 5c-wood (perhaps by adapting the 5-canonical decomposition introduced in [23])?

Question 4. Can 5c-orientations be used (e.g. using the framework of [2]) to have a bijective derivation of the generating function of 5-connected triangulations, expressed in [16]?

Question 5. Is there a nice counting formula for the total number of 5c-woods on 5c-triangulations with n inner vertices? (For Schnyder woods such a formula is $\frac{6(2n)!(2n+2)!}{n!(n+1)!(n+2)!(n+3)!}$ [5].)

References

1. O. Bernardi and É. Fusy. Schnyder decompositions for regular plane graphs and application to drawing. *Algorithmica*, 62(3):1159–1197, 2012.
2. O. Bernardi and É. Fusy. Unified bijections for maps with prescribed degrees and girth. *Journal of Combinatorial Theory, Series A*, 119:1351–1387, 2012.

3. O. Bernardi, É. Fusy, and S. Liang. Grand Schnyder woods. ArXiv preprint arXiv.2303.15630, 2023.
4. T. Biedl and G. Kant. A better heuristic for orthogonal graph drawings. *Comput. Geom. Theory Appl*, 9:159–180, 1998.
5. N. Bonichon. A bijection between realizers of maximal plane graphs and pairs of non-crossing Dyck paths. *Discrete Math.*, 298:104–114, 2005.
6. N. Bonichon, S. Felsner, and M. Mosbah. Convex drawings of 3-connected plane graphs. *Algorithmica*, 47(4):399–420, 2007.
7. M. Chrobak and G. Kant. Convex grid drawings of 3-connected planar graphs. *International Journal of Computational Geometry & Applications*, 7(03):211–223, 1997.
8. H. de Fraysseix, J. Pach, and R. Pollack. Small sets supporting Fáry embeddings of planar graphs. In *Proceedings of STOC*, pages 426–433. ACM, 1988.
9. É. Colin de Verdière. *Shortening of curves and decomposition of surfaces.* PhD thesis, Université Paris 7, 2003.
10. G. Di Battista, R. Tamassia, and L. Vismara. Output-sensitive reporting of disjoint paths. *Algorithmica*, 23(4):302–340, 1999.
11. S. Felsner. Convex drawings of planar graphs and the order dimension of 3-polytopes. *Order*, 18:19–37, 2001.
12. S. Felsner. Geodesic embeddings and planar graphs. *Order*, 20:135–150, 2003.
13. S. Felsner, H. Schrezenmaier, and R. Steiner. Pentagon contact representations. *Electronic Journal of Combinatorics*, 25(3):P3.39, 2018.
14. S. Felsner and F. Zickfeld. Schnyder woods and orthogonal surfaces. *Discrete & Computational Geometry*, 40(1):103–126, 2008.
15. É. Fusy. Transversal structures on triangulations: A combinatorial study and straight-line drawings. *Discrete Math.*, 309:1870–1894, 2009.
16. Z.J. Gao, I.M. Wanless, and N.C. Wormald. Counting 5-connected planar triangulations. *Journal of Graph Theory*, 38(1):18–35, 2001.
17. X. He. On finding the rectangular duals of planar triangulated graphs. *SIAM Journal on Computing*, 22:1218–1226, 1993.
18. X. He. Grid embedding of 4-connected plane graphs. *Discrete & Computational Geometry*, 17(3):339–358, 1997.
19. G. Kant and X. He. Regular edge labeling of 4-connected plane graphs and its applications in graph drawing problems. *Theoretical Computer Science*, 172:175–193, 1997.
20. E. Miller. Planar graphs as minimal resolutions of trivariate monomial ideals. *Documenta Mathematica 7 (2002), 43-90*, 7:43–90, 2002.
21. K. Miura. Grid drawings of five-connected plane graphs. *IEICE Transactions on Fundamentals of Electronics, Communications and Computer Sciences*, 105(9):1228–1234, 2022.
22. K. Miura, S. Nakano, and T. Nishizeki. Grid drawings of 4-connected plane graphs. *Discret. Comput. Geom.*, 26(1):73–87, 2001.
23. S. Nagai and S. Nakano. A linear-time algorithm to find independent spanning trees in maximal planar graphs. In *Graph-Theoretic Concepts in Computer Science: WG'2000*, pages 290–301, 2000.
24. W. Schnyder. Planar graphs and poset dimension. *Order*, 5(4):323–343, 1989.
25. W. Schnyder. Embedding planar graphs in the grid. *Symposium on Discrete Algorithms (SODA)*, pages 138–148, 1990.
26. R. Tamassia. On embedding a graph in a grid with the minimum number of bends. *SIAM Journal on Computing*, 16:421–444, 1987.
27. W.T. Tutte. How to draw a graph. *Proceedings of the London Mathematical Society*, 3(1):743–767, 1963.

A Appendix

In this appendix we prove Lemmas 2.4, 2.7, and Proposition 3.1. We also complete the proof of Theorem 2.8 by describing a linear time algorithm for constructing 5c-structures. Lastly, we prove that the complexity of the drawing algorithm is linear in the number of vertices.

A.1 Proof of Lemma 2.4

We start by proving an additional property of 5c-labelings.

Lemma A.1 *Let $\mathcal{L}$ be a 5c-labeling of a 5-triangulation G. For any inner edge e, the sum of label jumps between consecutive corners in counterclockwise order around e is equal to 5. This is represented in Figure 11.*

Proof. Note that for any inner vertex or any inner face x, the sum cw-jump(x) of label jumps between consecutive corners in clockwise order around x is equal to 5. For an inner edge e we denote by ccw-jump(e) the sum of label jumps between consecutive corners in counterclockwise order around e.

Observe that a clockwise label jump around an inner vertex or an inner face is either a counterclockwise label jump around an inner edge, or a label jump along an outer edge (and there are exactly 5 such jumps, each with value 1). Hence, $\sum_{f\in F}$ cw-jump$(f) + \sum_{v\in V}$ cw-jump$(v) = 5 + \sum_{e\in E}$ ccw-jump(e), where V, E, F are the sets of inner vertices, inner faces and inner edges, respectively. The left-hand side is equal to $5(|V|+|F|)$, which in turn is equal to $5+5|E|$ by the Euler relation. Since ccw-jump(e) must be a nonzero (by Condition (L2)) multiple of 5, it has to be exactly 5, for all $e \in E$. □

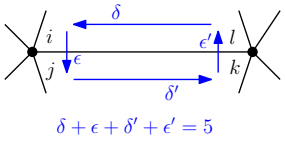

Fig. 11. Counterclockwise label jumps around an edge.

Now we prove Lemma 2.4. Let $\mathcal{L} \in \mathbf{L}_G$. We first show that $\Phi(\mathcal{L})$ is a 5c-orientation. Condition (O0) is a direct consequence of Condition (L0). Every inner primal vertex has outdegree 5 by Condition (L1), and every dual vertex has outdegree 2 by Condition (L2). Also, Lemma A.1 implies that every edge-vertex has outdegree 1. Hence, Condition (O1) holds, and $\Phi(\mathcal{L})$ is a 5c-orientation.

We now describe the inverse map. Let $\mathcal{O}$ be a 5c-orientation. The orientations of edges in $\mathcal{O}$ dictate the label jumps between consecutive corners around vertices

and faces. One can then follow these label jumps in order to propagate labels, starting from corners at the outer vertices (which are fixed by Condition (L0)) inward to all corners. If no conflict arises in this propagation (so that all the dictated label jumps are satisfied), then one obtains a labeling of corners $\mathcal{L}$, which we denote by $\overline{\Phi}(\mathcal{O})$. We prove below that, for any 5c-orientation $\mathcal{O}$, no conflict occurs during the propagation of labels, and that $\overline{\Phi}(\mathcal{O})$ is a 5c-labeling.

Consider the *corner graph* C_G of G defined as follows: C_G is a directed graph whose vertices are the inner corners of G, and there is an oriented edge from a corner c to a corner c' in C_G if c' is the corner following c in clockwise order around a face or a vertex. A corner graph is represented in Figure 12. C_G is naturally endowed with an embedding which is induced by the embedding of G (in fact C_G is obtained from the dual of G^+ by deleting a vertex). In particular, C_G has three types of inner faces, corresponding to inner vertices, inner edges and inner faces of G respectively.

We define the *$\mathcal{O}$-weight* $w(a)$ of an arc $a = (c, c')$ of C_G to be the label jump from c to c' determined by $\mathcal{O}$ according to the rules given by Figure 4(a). The *$\mathcal{O}$-weight* $w(P)$ of a directed path P of C_G is the sum of the $\mathcal{O}$-weight of the arcs of P. Note that the propagation rule causes no conflicts if and only if for any two (not necessarily consecutive) corners c and c' and any two directed paths P_1, P_2 in C_G from c to c', we have $w(P_1) \equiv w(P_2) \pmod 5$. To show the later property it suffices to show that for any simple cycle C in C_G, we have

$$\sum_{a \in C^+} w(a) - \sum_{a \in C^-} w(a) \equiv 0 \pmod 5,$$

where C^+ and C^- are the sets of arcs appearing clockwise and counterclockwise on C, respectively. It is easy to see that this holds if and only if the $\mathcal{O}$-weight of the contour of each inner face in C_G is congruent to 0 modulo 5. This last condition is implied by Condition (O1) of 5c-orientations. Hence the corner labeling $\mathcal{L} = \overline{\Phi}(\mathcal{O})$ is well-defined. Moreover $\mathcal{L}$ is indeed a 5c-labeling because Condition (L0) is satisfied by definition, and Conditions (L1) and (L2) are easy consequences of Condition (O1).

Finally, it is easy to see that Φ and $\overline{\Phi}$ are inverse to each other, hence they give bijections between 5c-labelings and 5c-orientations of G. This completes the proof of Lemma 2.4.

A.2 Proof of Lemma 2.7

Let $\mathcal{L}$ be a 5c-labeling of G. We first show that $\Theta(\mathcal{L})$ is a 5c-wood. By (L0), the arcs that start at outer vertices receive no color. Moreover, Conditions (L1) and (L2) and Lemma A.1 imply that for any inner edge $e = \{u, v\}$ with labels i on each side at v, the labels at u must be $i+2$ on the left and $i+3$ on the right, so that the arc (u, v) receives label i. This implies that the inner arcs ending at v_i receive color i by Θ. Hence $\Theta(\mathcal{L})$ satisfies (W0).

It is clear that (W1) is a direct consequence of (L1). To verify (W2), consider an inner arc $a = (u, v)$ of color $i \in [1 : 5]$, with v an inner vertex. Let $i+2, i+3, j, k$

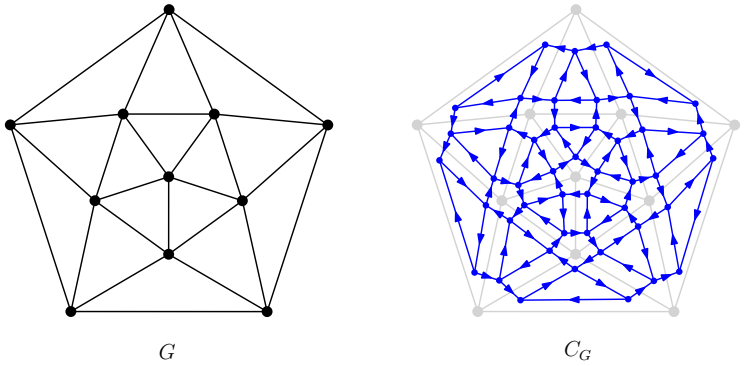

Fig. 12. A 5-triangulation G and its corner graph C_G.

be the labels in counterclockwise order around a, starting with those two incident to u. By (L2), $j \in \{i-1, i\}$ and $k \in \{i, i+1\}$. Therefore the opposite arc $-a$ has either no color while being between the arcs of colors $i+2$ and $i+3$ starting from v, or it has color $i+2$, or color $i+3$, which proves that the arc a satisfies (W2).

Lastly, for any inner edge $e = \{u, v\}$, Lemma A.1 and Conditions (L1) and (L2) easily imply that either 1 or 2 arcs of e receive a color (depending on having one or two label jumps equal to 2 along e, giving respectively two or one label jumps equal to 1 across e). Therefore $\Theta(\mathcal{L})$ satisfies (W3) and is a 5c-wood.

To prove that Θ is a bijection, we now describe the inverse map. Given a 5c-wood $\mathcal{W}$ on G, we define a corner labeling $\overline{\Theta}(\mathcal{W})$ as follows:

- the inner corners incident to the outer vertex v_i receive label i;
- a corner incident to an inner vertex v receives label i if it is between the outgoing arcs of colors $i+2$ and $i+3$ in clockwise order around v.

We need to show that $\overline{\Theta}(\mathcal{W})$ is indeed a 5c-labeling. Conditions (L0) and (L1) are clearly satisfied. Next we check that any label jump in clockwise direction around a face is equal to 1 or 2. Let $e = \{u, v\}$ be an inner edge of G. By (W3), one of its two arcs has some color i, say the one starting at u. Let $i+2, i+3, j, k$ be the labels of the corners in counterclockwise order around e, starting with those two incident to u. Then (W2) implies that $(j, k) \in \{(i-1, i), (i, i), (i, i+1)\}$. In all cases, the label jumps from $i+3$ to j and from k to $i+2$ are both in $\{1, 2\}$. Since the sum of label jumps in clockwise direction around a face is a multiple of 5, and each jump is in $\{1, 2\}$, the only possibility is that one label jump is equal to 1 and two label jumps are equal to 2. This shows that $\overline{\Theta}(\mathcal{W})$ satisfies (L2), hence is a 5c-wood.

Finally, it is clear that the mappings Θ and $\overline{\Theta}$ are inverse of each other, hence they give bijections between the sets of 5c-labelings and 5c-woods of G. This completes the proof of Lemma 2.7.

A.3 Proof of Theorem 2.8 and construction algorithm

In this subsection we complete the proof of Theorem 2.8. Let us first show that a 5-triangulation G admitting a 5c-orientation is necessarily a 5c-triangulation. If G admits a 5c-orientation, it also admits a 5c-wood $\mathcal{W} = (W_1, \ldots, W_5)$. For an inner vertex v of G, we consider the paths $P_i(v)$ in W_i from v to v_i, for $i \in [1:5]$. As we have seen in Section 3.1 (up to the forthcoming proof of Proposition 3.1), the paths $P_1(v), \ldots, P_5(v)$ have no vertex in common except v. Hence v cannot be in the interior of a simple cycle of length less than 5. This proves that G is a 5c-triangulation.

In the rest of this section, we describe a linear time algorithm for computing a 5c-orientation of a 5c-triangulation G. The process is illustrated in Figure 13, it uses some facts about *regular edge labelings*, which are combinatorial structures for triangulations of the 4-gon first defined by He in [17], and rediscovered in [15] under the name of *transversal structures*. We will rely on an incarnation of these structures as certain outdegree-constrained orientations. Let H be a triangulation of the 4-gon, and let $H^\diamond$ be the map obtained by placing a *face-vertex* in each inner face of H and joining it to the three vertices incident to this face (and then erasing the original edges of H).

A *regular orientation* of H is an orientation of $H^\diamond$ such that every face-vertex of $H^\diamond$ has outdegree 1 and every original inner vertex of H has outdegree 4; an example is shown in Figure 13(b). It follows from [17,15] that a triangulation of the 4-gon H admits a regular orientation if and only if H has no cycle of length less than 4 containing a vertex in its interior (equivalently, it has no loop nor multiple edges, and every 3-cycle is the boundary of a face). Moreover, such an orientation can be computed in linear time [19] (an independent proof is given in [3]).

Let G be a 5c-triangulation. Let H be the triangulation of the 4-gon obtained from G by placing a new vertex v_0 in the outer face of G and joining v_0 to v_1, v_2, v_3 and v_4. Since G is a 5c-triangulation, H has no cycle of length less than 4 containing a vertex in its interior. Hence, as recalled above, H admits a regular orientation $\mathcal{A}$, which can be computed in linear time. The situation is represented in Figure 13(a-b). Let $G^\diamond$ be the subgraph of $H^\diamond$ obtained by deleting the vertices and edges of $H^\diamond$ in the outer face of G. Consider the restriction $\mathcal{A}'$ of $\mathcal{A}$ to $G^\diamond$. Let b_i be the face-vertex of $G^\diamond$ in the inner face of G incident to the outer edge $\{v_i, v_{i+1}\}$ for $i \in [1:5]$. By definition, the face-vertex b_i has outdegree 1 in $\mathcal{A}'$, and we can reorient one of the edges $\{b_i, v_i\}$ or $\{b_i, v_{i+1}\}$ to obtain an orientation $\mathcal{B}$ of $G^\diamond$ such that

- for all $i \in [1:5]$, the face-vertex b_i has outdegree 2,
- the face-vertices of $G^\diamond$ distinct from $b_1, \ldots, b_5$ have outdegree 1,
- the original inner vertices of G have outdegree 4.

The orientation $\mathcal{B}$ of $G^\diamond$ is represented in Figure 13(c).

It is easy to check (using the Euler relation), that in $\mathcal{B}$ there is a unique oriented edge e_* of $G^\diamond$ whose initial vertex is an outer vertex of G. Let v_* be the initial vertex of e_*. One can show that the orientation $\mathcal{B}$ is *accessible from* v_*, that is, for every vertex of v of $G^\diamond$ there is a directed path from v_* to v in $\mathcal{B}$.

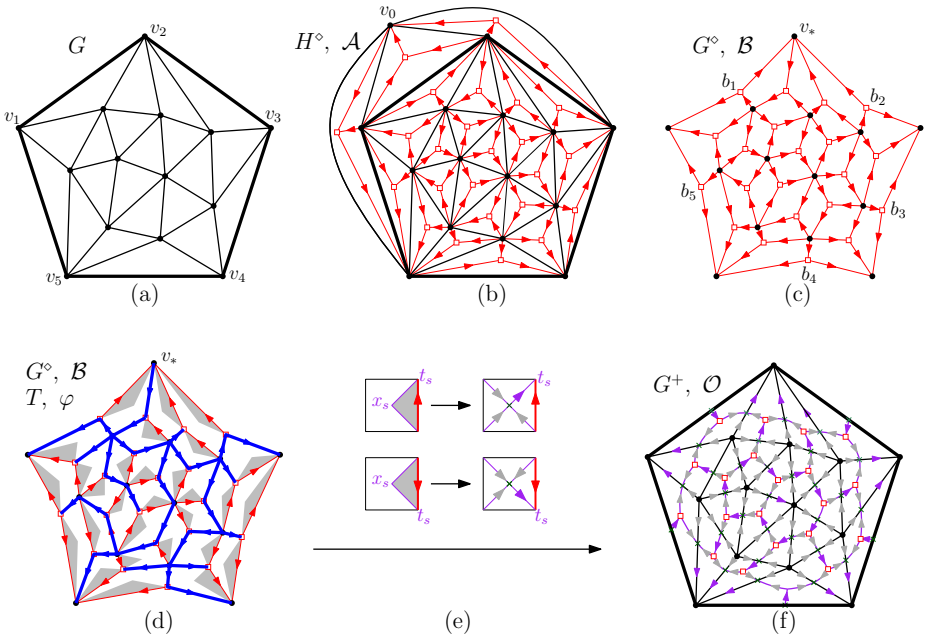

Fig. 13. Construction of a 5c-orientation for a 5c-triangulation. (a) A 5c-triangulation G. (b) The triangulation of the 4-gon H (obtained from G by placing a vertex v_0 in the outer face of G), and the regular orientation $\mathcal{A}$ of $H^\diamond$. (c) The orientation $\mathcal{B}$ of $G^\diamond$. (d) The spanning tree T (indicated by bold lines) oriented from the root vertex v_* to the leaves, and the bijection φ between the set S of inner faces of $G^\diamond$ and set $\overline{T}$ of edges not in T: for each edge e in $\overline{T}$, the corresponding face $\varphi(e)$ is indicated by a shaded triangle inside of $\varphi(e)$ and incident to e. (e) The rule (inside each inner face s of $G^\diamond$) for computing the orientation $\mathcal{O}$ of the primal-dual completion G^+. (f) The resulting 5c-orientation $\mathcal{O}$ of G^+.

We leave the proof of this accessibility property to the reader, and only mention that it relies on the fact that G has no cycle of length less than 5 containing a vertex in its interior. Since $\mathcal{B}$ is accessible from v_*, there exists a spanning tree T of $G^\diamond$ rooted at v_* and such that every edge of T is oriented from parent to children in $\mathcal{B}$. The spanning tree T is represented in Figure 13(d).

Next we use $\mathcal{B}$ and T to define an orientation $\mathcal{O}$ of the primal-dual completion G^+ of G. Let S be the set of inner faces of $G^\diamond$. By definition, S is in bijection with the inner edges of G, and the primal-dual completion G^+ of G is obtained by:

- adding an edge-vertex x_s in each inner face $s \in S$ and joining it to the 4 incident vertices of $G^\diamond$,
- adding an edge-vertex x_i for all $i \in [1:5]$ and joining it to v_i, v_{i+1} and b_i.

Let $\overline{T}$ be the set of edges of $G^\diamond$ not in T. It is classical (for any spanning tree T of a plane graph) that $\overline{T}$ is in bijection with the set S of inner face of

$G^\diamond$, where the bijection φ associates to an edge $e \in \overline{T}$ the face $\varphi(e) \in S$ incident to e and enclosed by the unique cycle in $T \cup \{e\}$. The bijection φ is indicated in Figure 13(d). For $s \in S$ we denote by t_s the terminal vertex of the edge $e \in \overline{T}$ such that $\varphi(e) = s$. We now orient G^+ by the following rule illustrated in Figure 13(e):

- for each face $s \in S$, the edge (x_s, t_s) is oriented toward t_s, while the 3 other edges incident to x_s are oriented toward x_s,
- for each $i \in [1:5]$, the edge (x_i, b_i) is oriented toward b_i.

The resulting orientation $\mathcal{O}$ of G^+ is indicated in Figure 13(f). One can check that $\mathcal{O}$ is a 5c-orientation of G: each edge-vertex has outdegree 1, each face-vertex has outdegree 2, and each inner original vertex has outdegree 5 (we leave the proof to the reader). Moreover, the operations required to go from the regular orientation $\mathcal{A}$ to the 5c-orientation $\mathcal{O}$ can clearly be performed in linear time. This concludes the proof of Theorem 2.8.

A.4 Proof of Proposition 3.1

Suppose for contradiction that $\mathcal{O}_i$ has a simple directed cycle. We put a partial order $\prec$ on the set of simple directed cycles of $\mathcal{O}_i$, by declaring $C \prec C'$ if the region enclosed by C is contained in the region enclosed by C'. Let C be a directed cycle of $\mathcal{O}_i$ which is minimal for this partial order.

Suppose first that there is a vertex v_0 in the region enclosed by C. For $j \in [1:5]$, let P_j be the directed path starting at v_0 and made of the arcs in W_j. This directed path P_j either ends at the outer vertex v_j or contains a directed cycle, but in either case it does not stay within the region enclosed by C (by minimality of C). Hence P_j contains a directed path P'_j from v_0 to a vertex of C. Hence $\mathcal{O}_i$ contains a directed path (going through v_0) from a vertex of C to a vertex of C: for instance, take the opposite of the path P'_{i-2} concatenated with the path P'_i. This contradicts the minimality of C, hence there is no vertex in the region enclosed by C.

Thus, still by minimality of C, there cannot be any edge enclosed by C (since every inner edge is oriented at least 1 way in $\mathcal{O}_i$). Hence C must be the contour of an inner face f of G. If C is a clockwise cycle, it is easy to see that the corners of f are labeled either $i-1$ or $i-2$ in the 5c-labeling $\overline{\Theta}(\mathcal{W})$ (because the corner at a vertex v of f must be incident to the arc of W_{i+1} with initial vertex v). But this is impossible since the 3 corners of f must have distinct labels in the 5c-labeling $\overline{\Theta}(\mathcal{W})$. Similarly, if C is a counterclockwise cycle, then the corners of f are all labeled either $i+1$ or $i+2$ in $\overline{\Theta}(\mathcal{W})$, which is impossible.

This completes the proof that $\mathcal{O}_i$ is acyclic. The second statement in Proposition 3.1 follows immediately, which completes the proof.

A.5 Time complexity

In this subsection we explain how the 5c-barycentric drawing algorithm can be performed in a number of operations which is linear in the number of vertices. The proof follows the same line as for Schnyder's classical algorithm.

First recall from Theorem 2.8 that for a 5c-triangulation G with n vertices, a 5c-wood $\mathcal{W} = (W_1, \ldots, W_5)$ can be computed in $O(n)$ operations. As we now explain, the regions' sizes $|R_i(v)|$ for all inner vertices v and $i \in [1:5]$ can also be computed in $O(n)$ operations, hence the total time-complexity of the drawing algorithm is $O(n)$.

The computation below is based on the following observation: for an inner vertex v, the vertices strictly inside the region $R_i(v)$ are all the descendants in the tree W_i of the inner vertices on the paths $P_{i-2}(v)$ and $P_{i+2}(v)$ (excluding the vertices on the paths $P_{i-2}(v)$ and $P_{i+2}(v)$). Let V be the set of inner vertices of G. For $v \in V$ and $i \in [1:5]$, let $N_i(v)$ be the number of descendants of v in W_i (with v not considered a descendant of itself). The list $\{N_i(v),\ v \in V\}$ can be computed in $O(n)$ operations proceeding from leaves to root, that is, starting from the set L of leaves of W_i, then the set of leaves of $W_i \backslash L$, etc. For $j \in \{i-2, i+2\}$, we let $N_i^j(v)$ be $N_i(w) + 1$ if v has a child w in W_i such that the arc (v, w) has color j (such a child is necessarily unique by Condition (W2) of 5c-woods), and be 0 otherwise. Clearly the list $\{N_i^j(v),\ v \in V\}$ can be computed in $O(n)$ operations. Once all these lists are computed, for $i \in [1:5]$ and $v \in V$, and with the notation $P'_k(v) = P_k(v) \backslash \{v, v_k\}$, we let $N_i^{\text{left}}(v) = \sum_{u \in P'_{i-2}(v)} (N_i(u) - N_i^{i-2}(u))$, and $N_i^{\text{right}}(v) = \sum_{u \in P'_{i+2}(v)} (N_i(u) - N_i^{i+2}(u))$. The list $\{N_i^{\text{left}}(v),\ v \in V\}$ (resp. $\{N_i^{\text{right}}(v),\ v \in V\}$) can again be computed in $O(n)$ operations, here proceeding from root to leaves in W_{i-2} (resp. in W_{i+2}). Then, for $v \in V$, the above observation implies that the number $n_i(v)$ of vertices strictly inside $R_i(v)$ is

$$n_i(v) = \big(N_i(v) - N_i^{i-2}(v) - N_i^{i+2}(v)\big) + N_i^{\text{left}}(v) + N_i^{\text{right}}(v).$$

One can also compute the list $\{\text{length}(P_i(v)),\ v \in V\}$ in $O(n)$ operations (proceeding from root to leaves in W_i). By the Euler relation the number of faces $|R_i(v)|$ is $2n_i(v) + \text{length}(P_{i-2}(v)) + \text{length}(P_{i+2}(v)) - 1$. Hence the list $\{|R_i(v)|,\ v \in V\}$ can be computed in $O(n)$ operations, as claimed.